Protein overexpression of *HER2* by malignant CMTs has been reported in several studies. However, there was no difference in *HER2* expression between benign and malignant or between non-invasive and invasive CMTs. Ahern *et al.* reported overexpression of *HER2* mRNA in 17 of 23 malignant CMTs, but in none of 5 benign CMTs [1]. A recent study reported no differences in the *HER2* mRNA levels between adenomas and carcinomas or between presence and absence of lymph node involvement of CMTs [23]. In human breast cancer, reports on the interaction between mRNA expression and HER2 protein or DNA amplification levels did not reach agreement [5, 13]. Since there was no significant difference in *HER2* expression among CMT tissue samples in the present study, *HER2* was not assessed in FNB samples.

This study investigated the mRNA expressions of *SATB1* and *Snail* in CMT tissue, and expressions of both *SATB1* and *Snail* were clearly higher in invasive CMTs than in non-invasive CMTs. One sample which expressed remarkably high *SATB1* or *Snail* might influence on the statistical analysis. However, the each sample was not excluded from the analysis because of their association with clinical features. The tissue sample expressing very high *SATB1* was obtained from the invasive CMT with involved lymph node and the skin metastasis were occurred two months after the operation. The other CMT expressing high very *Snail* was osteosarcoma with vascular invasion, and their aggressive behaviors have been generally known [27]. Further, other samples with high level of *SATB1* correlated with a poor clinical outcome. Moreover, comparison of the amino acid sequence of canine and human SATB1 showed that two important domains of canine SATB1 for DNA binding and homodimerization had 100% similarity to human SATB1 (data not shown). These results suggest that the canine SATB1 may also regulate tumor metastasis genes, such as Snail, to make tumor cells a more aggressive phenotype, as in human breast cancer. However, in the FNB samples, no differences in the expression levels of *SATB1* and *Snail* between invasive CMTs and non-invasive CMTs were detected. The cause of this result might be the possibility that small amounts of tumor cells express *SATB1* and *Snail*. Recent studies in human based on the expression of EMT markers reported that EMT occurred in a more local region at the invasive area of the tumor [8]. It might be difficult to collect *SATB1* and *Snail*-expressing tumor cells in the limited area sampled by FNB.

On discriminant analysis using gene expression levels of *ER*, *PR*, *SATB1*, and *Snail*, 73.2% of all tissue samples were correctly classified as benign or malignant CMTs, and 80.0% of all tissue samples were correctly classified as non-invasive or invasive CMTs. In FNB samples, expression levels of *ER* and *PR* had a high positive correlation to those in tissue samples. *ER* and *PR* might be suitable biomarkers for cytological gene examination. In addition, using gene expression levels of *ER* and *PR*, the accuracy of 74.2% for tumor classification according to malignancy was as the same as for tissue samples, and that for invasiveness (71.0%) was slightly lower. Aleen *et al.* reported that the accuracies of cytological examinations of FNB samples of CMTs by two cytologists were 79% and 66% [2]. It is interesting that FNB samples could be correctly classified as benign or malignant CMTs only by *ER* and *PR* levels with a similar accuracy to the report by Aleen *et al.* However, investigation of more gene expressions that can be detected even in FNB samples is needed to improve the accuracy of cytological gene examination. In this study, there were high percentages of false-positive (number of benign samples diagnosed as malignant) results in tissue and FNB samples (46 and 38%, respectively). Considering the report that concentrations of ER and PR in CMTs tended to vary with estrous cycle stage [15], it might be a difficult to classify benign or malignant CMTs with 100% accuracy only by *ER* and *PR* levels. In the future, use of other genes related to malignancy or, currently, referral for cytological examination might improve the accuracy of FNB samples. mRNA quantification of FNB samples by qRT-PCR cost much money and time, so that a simple gene examination kit should be considered.

In conclusion, the present study suggested that *ER* and *PR* are reliable biomarkers for the gene examination of FNB samples, and canine *SATB1* and *Snail* might have a role in tumor progression, as in humans. Cytological gene examination could become a useful diagnostic tool that can be performed easily without anesthesia and could predict tumor malignancy and invasiveness prior to surgical removal. To establish cytological gene examination of CMTs, more studies of gene expressions, including key biomarkers that are widely involved in the tumor mechanism, are needed.

REFERENCES

1. Ahern, T. E., Bird, R. C., Bird, A. E. and Wolfe, L. G. 1996. Expression of the oncogene c-erbB-2 in canine mammary cancers and tumor-derived cell lines. *Am. J. Vet. Res.* **57**: 693–696. [Medline]
2. Allen, S. W., Prasse, K. W. and Mahaffey, E. A. 1986. Cytologic differentiation of benign from malignant canine mammary tumors. *Vet. Pathol.* **23**: 649–655. [Medline]
3. Almasri, N. M. and Al Hamad, M. 2005. Immunohistochemical evaluation of human epidermal growth factor receptor 2 and estrogen and progesterone receptors in breast carcinoma in Jordan. *Breast Cancer Res.* **7**: R598–R604. [Medline] [CrossRef]
4. Alvarez, J. D., Yasui, D. H., Niida, H., Joh, T., Loh, D. Y. and Kohwi-Shigematsu, T. 2000. The MAR-binding protein SATB1 orchestrates temporal and spatial expression of multiple genes during T-cell development. *Genes Dev.* **14**: 521–535. [Medline]
5. Barberis, M., Pellegrini, C., Cannone, M., Arizzi, C., Coggi, G. and Bosari, S. 2008. Quantitative PCR and HER2 testing in breast cancer: a technical and cost-effectiveness analysis. *Am. J. Clin. Pathol.* **129**: 563–570. [Medline] [CrossRef]
6. Batlle, E., Sancho, E., Francí, C., Domínguez, D., Monfar, M., Baulida, J. and García de Herreros, A. 2000. The transcription factor snail is a repressor of E-cadherin gene expression in epithelial tumour cells. *Nat. Cell Biol.* **2**: 84–89. [Medline] [CrossRef]
7. Blanco, M. J., Moreno-Bueno, G., Sarrio, D., Locascio, A., Cano, A., Palacios, J. and Nieto, M. A. 2002. Correlation of Snail expression with histological grade and lymph node sta-

tus in breast carcinomas. *Oncogene* **21**: 3241–3246. [Medline] [CrossRef]
8. Brabletz, T., Jung, A., Reu, S., Porzner, M., Hlubek, F., Kunz-Schughart, L. A., Knuechel, R. and Kirchner, T. 2001. Variable beta-catenin expression in colorectal cancers indicates tumor progression driven by the tumor environment. *Proc. Natl. Acad. Sci. U.S.A.* **98**: 10356–10361. [Medline] [CrossRef]
9. Brodey, R. S., Goldschmidt, M. H. and Roszel, J. R. 1983. Canine mammary gland neoplasms. *J. Am. Anim. Hosp. Assoc.* **19**: 61–90.
10. Cai, S., Han, H. J. and Kohwi-Shigematsu, T. 2003. Tissue-specific nuclear architecture and gene expression regulated by SATB1. *Nat. Genet.* **34**: 42–51. [Medline] [CrossRef]
11. Chang, C. C., Tsai, M. H., Liao, J. W., Chan, J. P., Wong, M. L. and Chang, S. C. 2009. Evaluation of hormone receptor expression for use in predicting survival of female dogs with malignant mammary gland tumors. *J. Am. Vet. Med. Assoc.* **235**: 391–396. [Medline] [CrossRef]
12. Cheng, C., Lu, X., Wang, G., Zheng, L., Shu, X., Zhu, S., Liu, K., Wu, K. and Tong, Q. 2010. Expression of SATB1 and heparanase in gastric cancer and its relationship to clinicopathologic features. *APMIS* **118**: 855–863. [Medline] [CrossRef]
13. Cuadros, M., Talavera, P., López, F. J., García-Peréz, I., Blanco, A. and Concha, A. 2010. Real-time RT-PCR analysis for evaluating the Her2/neu status in breast cancer. *Pathobiology* **77**: 38–45. [Medline] [CrossRef]
14. de Las Mulas, J. M., Millán, Y. and Dios, R. 2005. A prospective analysis of immunohistochemically determined estrogen receptor alpha and progesterone receptor expression and host and tumor factors as predictors of disease-free period in mammary tumors of the dog. *Vet. Pathol.* **42**: 200–212. [Medline] [CrossRef]
15. Donnay, I., Rauïs, J., Devleeschouwer, N., Wouters-Ballman, P., Leclercq, G. and Verstegen, J. 1995. Comparison of estrogen and progesterone receptor expression in normal and tumor mammary tissues from dogs. *Am. J. Vet. Res.* **56**: 1188–1194. [Medline]
16. Dutra, A. P., Granja, N. V., Schmitt, F. C. and Cassali, G. D. 2004. c-erbB-2 expression and nuclear pleomorphism in canine mammary tumors. *Braz. J. Med. Biol. Res.* **37**: 1673–1681. [Medline] [CrossRef]
17. Gilbertson, S. R., Kurzman, I. D., Zachrau, R. E., Hurvitz, A. I. and Black, M. M. 1983. Canine mammary epithelial neoplasms: biologic implications of morphologic characteristics assessed in 232 dogs. *Vet. Pathol.* **20**: 127–142. [Medline]
18. Han, H. J., Russo, J., Kohwi, Y. and Kohwi-Shigematsu, T. 2008. SATB1 reprogrammes gene expression to promote breast tumour growth and metastasis. *Nature* **452**: 187–193. [Medline] [CrossRef]
19. Hashimoto, S., Yamamura, H., Sato, T., Kanayama, K. and Sakai, T. 2002. The progression of canine mammary tumors and the concentrations of estrogen and progesterone receptors in the tumor tissues. *J. Anim. Clin. Med.* **11**: 163–166.
20. Hsu, W. L., Huang, H. M., Liao, J. W., Wong, M. L. and Chang, S. C. 2009. Increased survival in dogs with malignant mammary tumours overexpressing HER-2 protein and detection of a silent single nucleotide polymorphism in the canine HER-2 gene. *Vet. J.* **180**: 116–123. [Medline] [CrossRef]
21. Kanae, Y., Endoh, D., Yokota, H., Taniyama, H. and Hayashi, M. 2006. Expression of the PTEN tumor suppressor gene in malignant mammary gland tumors of dogs. *Am. J. Vet. Res.* **67**: 127–133. [Medline] [CrossRef]
22. Kim, J. H., Im, K. S., Kim, N. H., Yhee, J. Y., Nho, W. G. and Sur, J. H. 2011. Expression of HER-2 and nuclear localization of HER-3 protein in canine mammary tumors: histopathological and immunohistochemical study. *Vet. J.* **189**: 318–322. [Medline] [CrossRef]
23. Klopfleisch, R., Klose, P. and Gruber, A. D. 2010. The combined expression pattern of BMP2, LTBP4, and DERL1 discriminates malignant from benign canine mammary tumors. *Vet. Pathol.* **47**: 446–454. [Medline] [CrossRef]
24. Kumar, P. P., Bischof, O., Purbey, P. K., Notani, D., Urlaub, H., Dejean, A. and Galande, S. 2007. Functional interaction between PML and SATB1 regulates chromatin-loop architecture and transcription of the MHC class I locus. *Nat. Cell Biol.* **9**: 45–56. [Medline] [CrossRef]
25. Martin de las Mulas, J., Ordás, J., Millán, Y., Fernández-Soria, V. and Ramón y Cajal, S. 2003. Oncogene HER-2 in canine mammary gland carcinomas: an immunohistochemical and chromogenic in situ hybridization study. *Breast Cancer Res. Treat.* **80**: 363–367. [Medline]
26. Millanta, F., Calandrella, M., Bari, G., Niccolini, M., Vannozzi, I. and Poli, A. 2005. Comparison of steroid receptor expression in normal, dysplastic, and neoplastic canine and feline mammary tissues. *Res. Vet. Sci.* **79**: 225–232. [Medline] [CrossRef]
27. Misdorp, W., Cotchin, E., Hampe, J. F., Jabara, A. G. and von Sandersleben, J. 1971. Canine malignant mammary tumours. I. Sarcomas. *Vet. Pathol.* **8**: 99–117. [Medline]
28. Misdorp, W., Else, R. W., Hellmén, E. and Lipscomb, T. P. 1999. Histological Classification of Mammary Tumors of the Dog and Cat, 2nd Series, Vol.VII. WHO International Histological Classification of Mammary Tumors of Domestic Animals, AFIP, Washington, DC.
29. Olmeda, D., Moreno-Bueno, G., Flores, J. M., Fabra, A., Portillo, F. and Cano, A. 2007. SNAI1 is required for tumor growth and lymph node metastasis of human breast carcinoma MDA-MB-231 cells. *Cancer Res.* **67**: 11721–11731. [Medline] [CrossRef]
30. Perez, E. A., Roche, P. C., Jenkins, R. B., Reynolds, C. A., Halling, K. C., Ingle, J. N. and Wold, L. E. 2002. HER2 testing in patients with breast cancer: poor correlation between weak positivity by immunohistochemistry and gene amplification by fluorescence in situ hybridization. *Mayo Clin. Proc.* **77**: 148–154. [Medline]
31. Qiu, C., Lin, D. D., Wang, H. H., Qiao, C. H., Wang, J. and Zhang, T. 2008. Quantification of VEGF-C expression in canine mammary tumours. *Aust. Vet. J.* **86**: 279–282. [Medline] [CrossRef]
32. Slamon, D. J., Clark, G. M., Wong, S. G., Levin, W. J., Ullrich, A. and McGuire, W. L. 1987. Human breast cancer: correlation of relapse and survival with amplification of the HER-2/neu oncogene. *Science* **235**: 177–182. [Medline] [CrossRef]
33. Yang, J., Mani, S. A., Donaher, J. L., Ramaswamy, S., Itzykson, R. A., Come, C., Savagner, P., Gitelman, I., Richardson, A. and Weinberg, R. A. 2004. Twist, a master regulator of morphogenesis, plays an essential role in tumor metastasis. *Cell* **117**: 927–939. [Medline] [CrossRef]
34. Zavlaris, M., Angelopoulou, K., Vlemmas, I. and Papaioannou, N. 2009. Telomerase reverse transcriptase (TERT) expression in canine mammary tissues: a specific marker for malignancy? *Anticancer Res.* **29**: 319–325. [Medline]
35. Zhao, X. D., Ji, W. Y., Zhang, W., He, L. X., Yang, J., Liang, H. J. and Wang, L. L. 2010. Overexpression of SATB1 in laryngeal squamous cell carcinoma. *ORL J. Otorhinolaryngol. Relat. Spec.* **72**: 1–5. [Medline] [CrossRef]

Supplemental Table 1. Patients' characteristics

		n
Breed	Miniature Dachshund	14
	Shih Tzu	6
	Beagle	4
	Maltese	3
	Papillon	3
	Shetland Sheepdog	3
	American Cocker Spaniel	2
	Miniature Schnauzer	2
	Welsh Corgi Penbrakes	2
	West Highland White Terrier	2
	Cavalier King Charles Spaniel	2
	Great Pyrenees	1
	Poodle	1
	Chihuahua	1
	Japanese Spitz	1
	Miniature Bull Terrier	1
	Mixed Breed	7
Sex	Female (intact)	39
	Female (spayed)	15
	Male	1

		n
Tumor size	mean ± SD	2.9 ± 2.6 cm
	median	2 cm
	range	0.5 to 11 cm
	T1 (<3 cm)	30
	T2 (3–5 cm)	15
	T3 (>5 cm)	5
	unknown	6
Tumor type	Benign	
	Simple adenoma	2
	Complex adenoma	18
	Benign mixed tumor	8
	Malignant	
	Simple carcinoma	12
	Complex carcinoma	13
	Adenocarcinoma	1
	Carcinosarcoma	1
	Osteosarcoma	1
Age	mean±SD	10 ± 2.7 years
	median	10 years
	range	4 to 16 years

The Journal of Toxicological Sciences (J. Toxicol. Sci.)
Vol.37, No.2, 373-380, 2012

Original Article

Development of humanized steroid and xenobiotic receptor mouse by homologous knock-in of the human steroid and xenobiotic receptor ligand binding domain sequence

Katsuhide Igarashi[1], Satoshi Kitajima[1], Ken-ichi Aisaki[1], Kentaro Tanemura[1], Yuhji Taquahashi[1], Noriko Moriyama[1], Eriko Ikeno[1], Nae Matsuda[1], Yumiko Saga[2,3], Bruce Blumberg[4] and Jun Kanno[1]

[1]Division of Cellular and Molecular Toxicology, Biological Safety Research Center, National Institute of Health Sciences, 1-18-1 Kamiyoga, Setagaya-ku, Tokyo, 158-8501, Japan
[2]Division of Mammalian Development, National Institute of Genetics, Yata 1111, Mishima 411-8540, Japan
[3]The Graduate University for Advanced Studies (Sokendai), Yata 1111, Mishima 411-8540, Japan
[4]Department of Developmental and Cell Biology, 2011 Biological Sciences 3, University of California, Irvine, CA 92697-2300, USA

(Received December 7, 2011; Accepted January 12, 2012)

ABSTRACT — The human steroid and xenobiotic receptor (SXR), (also known as pregnane X receptor PXR, and NR1I2) is a low affinity sensor that responds to a variety of endobiotic, nutritional and xenobiotic ligands. SXR activates transcription of Cytochrome P450, family 3, subfamily A (CYP3A) and other important metabolic enzymes to up-regulate catabolic pathways mediating xenobiotic elimination. One key feature that demarcates SXR from other nuclear receptors is that the human and rodent orthologues exhibit different ligand preference for a subset of toxicologically important chemicals. This difference leads to a profound problem for rodent studies to predict toxicity in humans. The objective of this study is to generate a new humanized mouse line, which responds systemically to human-specific ligands in order to better predict systemic toxicity in humans. For this purpose, the ligand binding domain (LBD) of the human SXR was homologously knocked-in to the murine gene replacing the endogenous LBD. The LBD-humanized chimeric gene was expressed in all ten organs examined, including liver, small intestine, stomach, kidney and lung in a pattern similar to the endogenous gene expressed in the wild-type (WT) mouse. Quantitative reverse transcription-polymerase chain reaction (RT-PCR) analysis showed that the human-selective ligand, rifampicin induced Cyp3a11 and Carboxylesterase 6 (Ces6) mRNA expression in liver and intestine, whereas the murine-selective ligand, pregnenolone-16-carbonitrile did not. This new humanized mouse line should provide a useful tool for assessing whole body toxicity, whether acute, chronic or developmental, induced by human selective ligands themselves and subsequently generated metabolites that can trigger further toxic responses mediated secondarily by other receptors distributed body-wide.

Key words: Steroid and xenobiotic receptor, Pregnane X receptor, Humanized mouse, Ligand binding domain, Knock-in mouse

INTRODUCTION

Most orally administered xenobiotics are metabolized first by the intestine and then by the liver after portal transport. The expression levels of enzymes involved in xenobiotic metabolism are regulated at the transcriptional level by key xenobiotic sensors including the steroid and xenobiotic receptor (SXR), also known as the pregnane X receptor (PXR), pregnane activated receptor (PAR) and NR1I2 (Bertilsson *et al.*, 1998; Lehmann *et al.*, 1998; Blumberg *et al.*, 1998). SXR is important in the field of toxicology for at least two reasons. Firstly, this receptor system induces the expression of CYP3A and CYP2B enzymes, the major metabolizers of pharmaceu-

Correspondence: Jun Kanno (E-mail: kanno@nihs.go.jp)

ticals and xenobiotics. Therefore, SXR is a key mediator of drug- and chemical-induced toxicity as well as drug-drug and drug-nutrient interactions (Zhou *et al.*, 2004). Secondly, the orthologous rodent and human receptors exhibit differential sensitivity for a subset of chemical ligands important in the field of toxicology. For example, rifampicin (RIF) is a specific and selective activator of human SXR, whereas pregnenolone 16a-carbonitrile (PCN) is selective for the rodent orthologue.

Rodent-human differences in CYP3A and CYP2B-mediated responses to xenobiotics can be a profound problem in toxicologic studies where rodents are used to predict the toxicity of a compound in humans (Ma *et al.*, 2007). Therefore, development of a murine model that reconstructs the SXR-mediated systemic response of humans is of a great significance in toxicology.

Human and rodent SXRs share ~95% amino acid sequence identity in the DNA-binding domain (DBD) but only about 77% identity in the LBD. Tirona *et al.* (2004) analyzed the ligand selectivity of a human-rat chimeric protein and showed that the species differences are primarily defined by sequence differences in the LBD. Watkins and colleagues showed that the key residues responsible for the majority of the ligand selectivity were Leu 308 (human) and Phe305 (rat and mouse). Crystallographic analysis located these amino acids within or neighboring the flexible loop that forms a part of the pore to the ligand-binding cavity. Swapping the rodent and human-specific residues was shown to modulate the activation by the human-selective activator RIF *in vitro* (Watkins *et al.*, 2001). According to those findings, a simple replacement of the mouse LBD with the human sequence should be sufficient to "humanize" the ligand binding properties as well as activation of the downstream target genes.

Three kinds of humanized mice have already been generated. One is the SXR-null/Alb-SXR mouse (Alb-SXR mouse) made by crossing the SXR knockout mice with a transgenic mouse line that expresses human SXR in liver under the control of the albumin promoter (Xie *et al.*, 2000). Gonzalez and colleagues generated a transgenic mouse expressing a human BAC containing the entire hSXR gene in a SXR null background, thus controlled under human SXR promoter (SXR BAC mouse) (Ma *et al.*, 2007). Another mouse is the human SXR genome knock-in mice (hSXR genome mouse) (Scheer *et al.*, 2008). The human SXR genomic region from exon 2 to exon 9 was knocked-in to mouse SXR exon 2. This mouse expresses the human full length SXR mRNA under the control of mouse SXR promoter regulation. Although useful for toxicology studies, these mice have disadvantages in that the human SXR is expressed only in the liver (Alb-SXR mouse), hSXR mRNA is not expressed in all of the tissues where SXR is known to be expressed (SXR BAC mouse), and there might be potential differences in the binding affinities of hSXR DNA-binding domain (DBD) to *cis*-acting elements in mouse SXR target genes (hSXR genome mouse).

As noted above, it is known that the critical differences between human and rodent ligand-selectivity reside in the LBD. Therefore, when our project to generate a humanized SXR mouse was initiated, we reasoned that altering the LBD would be sufficient to generate a humanized ligand selectivity. We decided to retain the mouse DBD to avoid any potential differences between the binding affinities of the chimeric receptor for cis-acting elements in the mouse genome. To maintain the tissue-specific expression pattern of the endogenous gene, we inserted the human cDNA encoding the region carboxyl-terminal to the DBD into the mouse gene. This retains all of the 5' and 3' regulatory elements in the mouse gene, as well as introns 1 and 2, which contain important elements for regulating SXR expression (Jung *et al.*, 2006).

Here we report a new line of mouse (hSXRki mouse) in which a cDNA encoding the human LBD is homologously recombined into the mouse gene after exon 3. The tissue distribution of the resulting chimeric mouse DBD-human LBD mRNA is comparable to that of the WT mouse. The hSXRki mouse showed a fully humanized response to the human-selective activator RIF in that the Cyp3a11 mRNA was induced in liver and mucosa of small intestine in response to RIF, but not the rodent-selective compound PCN. This new mouse line should provide a useful tool for assessing the whole body toxicity induced by a human selective SXR ligand itself and its subsequently generated metabolite(s) that can trigger further toxic responses through other pathways body-wide.

MATERIALS AND METHODS

Generation of hSXRki knock-in mice

A DNA fragment of mouse SXR intron 2 to exon 3 was PCR amplified using mouse BAC DNA (BAC clone No. RP23-351P21) as a template. Primers used were BAC39486FW and mSXR462RV (for sequences of the primers see Table1). This fragment was connected to the LBD of human SXR cDNA from amino acid 105 through the carboxyl terminus amplified by the PCR primers: hSXR904FW and hSXR1887RVEcoRI (template; human SXR cDNA). The 3'UTR of bovine growth hormone (BGH) was added to 3' to the terminal codon. This concatenated fragment was introduced to a vector, which

Table 1. List of primer pairs

Purpose	Primer name	Sequence (5' to 3')
Targeting vector construction	BAC39486FW	CCATGGGTACCACGAATAACAA
	mSXR462RV	CATGCCACTCTCCAGGCA
	hSXR904FW	AAGAAGGAGATGATCATGTCCG
	hSXR1887RVEcoRI	CCGAATTCTCATCATCAGCTACCTGTGATACCGAACA
Genotyping	NeoAL2	GGGGATGCGGTGGGCTCTATGGCTT
	SXR RC RV5	TGAGAGTGCACAAGTTCAAGCT
	WTInt5	AGTGATGGGAACCACTCCTG
	WTEx6RV	TGGTCCTCAATAGGCAGGTC
	mhSXRE4	GTGAACGGACAGGGACTCAG
	mhSXRSARV	CTCTCCTGGCTCATCCTCAC
Percellome quantitative RT-PCR	Cyp3a11 FW	CAGCTTGGTGCTCCTCTACC
	Cyp3a11 RV	TCAAACAACCCCCATGTTTT
	Ces6 FW	GGAGCCTGAGTTCAGGACAGAC
	Ces6 RV	ACCCTCACTGTTGGGGTTC
	mouse SXR FW	AATCATGAAAGACAGGGTTC
	mouse SXR RV	AAGAGCACAGATCTTTCCG
	human SXR FW	ATCACCCGGAAGACACGAC
	human SXR RV	AAGAGCACAGATCTTTCCG
	mouse-human SXR FW	CCCATCAACGTAGAGGAGGA

has the neomycin resistance gene with loxP sequence at both ends, removable with Cre recombinase (Saga *et al.*, 1999). A 7kb KpnI fragment containing intron 2 was used as a long arm and 1.3kb PstI-EcoRI fragment containing from exon 8 to intron 8 was used as a short arm for homologous recombination (Fig. 1). The resulting targeting vector was linearized with SacII and introduced by electroporation to TT2 ES cell line (Yagi *et al.*, 1993) and neomycin resistant clones were selected, PCR genotyped, and confirmed by the Southern blotting. For generation of chimeric mice, these ES clones were aggregated with ICR 8-cell embryos and transferred to pseudopregnant female recipients. The chimeric mice born were bred with ICR females. Germ line transmission of the targeted allele was confirmed by PCR. A mouse was crossed with a CAG-Cre transgenic mouse (Sakai and Miyazaki, 1997) to evict the neomycin resistance gene, and back crossed to C57BL/6 CrSlc (SLC, Inc., Shizuoka, Japan) at least 6 generations and used for the analysis.

PCR Genotyping (See Table 1 for primer sequences)

Primers for identification of homologously recombined ES clones were NeoAL2 and SXR RC RV5. DNA purified from the tail of each mouse was used for PCR genotying. Primers for WT detection were WTInt5 and WTEx6RV amplifying a product of 755 bp. Primers for confirmation of removal of the neomycin resistance gene were mhSXRE4 and mhSXRSARV amplifying a product of 1,223 bp.

Southern blot analysis

To confirm homologous recombination, DNA from ES cell cultures was purified and digested with BamHI and XhoI, then electrophoresed and analyzed by Southern hybridization (Saga *et al.*, 1997). Mouse SXR exon 9 region which remains after homologous recombination was used for the probe. The restriction fragments from the WT allele and targeted allele are 2,305 bp and 1,925 bp, respectively.

Chemicals

RIF (molecular weight 822.95) and PCN (molecular weight 341.49) were purchased from Sigma-Aldrich (St. Louis, MO, USA). Corn oil was purchased from Wako Pure Chemical Industries (Osaka, Japan).

Quantitative RT-PCR (Percellome PCR) (See Table 1 for primer sequences)

The method for Percellome quantitative RT-PCR was described previously (Kanno *et al.*, 2006). Briefly, tissue pieces stored in RNAlater (Ambion, Austin, TX, USA) were homogenized and lysed in RLT buffer (Qiagen GmbH., Germany) and 10 μl aliquots were used

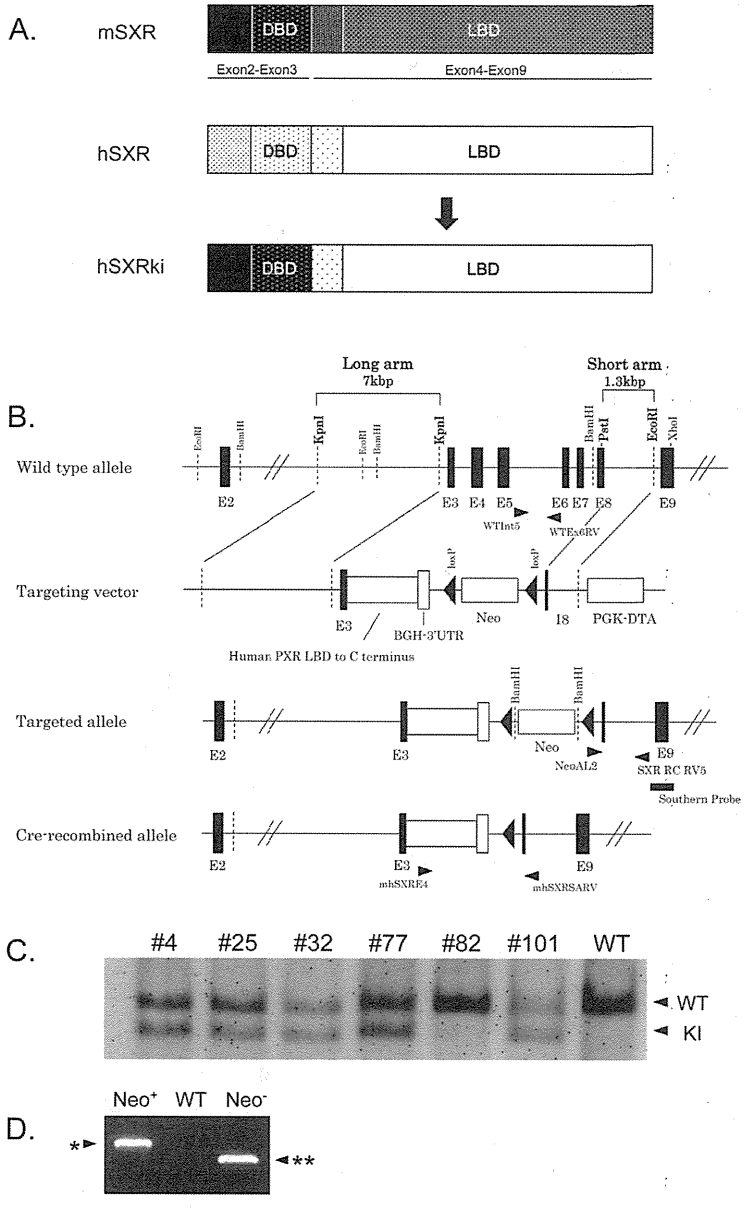

Fig. 1. Targeting strategy used to generate the hSXRki mouse. A) Diagram of hSXRki chimeric protein. Hinge region and ligand binding domain (LBD) of human SXR are knocked-in to mouse SXR, resulting in chimeric protein having murine N-ternial domain and DNA binding domain (DBD). B) Targeting strategy used to generate the hSXRki mouse. The chimeric mouse DBD and human LBD fragment, followed by the BGH 3' UTR were knocked-in to the mouse SXR gene. The genomic region spanning from exon 3 to exon 8 was substituted by the inserted fragment with the remainder of the gene remaining intact. C) Confirmation of homologous recombination by southern blot analysis. Six ES clones positive for recombination by PCR genotyping were further analyzed by southern blot (clones #4 ~ #101). Lower bands (1925 bp) indicate successful homologous recombination; upper bands (2305 bp) correspond to WT allele. Clones #4, #25, #32, #77 and #101 were confirmed as homologous recombinants; clones #4 and #25 were used for the generation of chimeric mice. D) Confirmation of Cre-mediated removal of the neomycin resistance gene. Mouse tail genome DNA was PCR amplified with the primer set, mhSXRE4 and mhSXRSARV. *: 2,858 bp (for the mice having the neomycin resistance gene), **: 1,223 bp (for the mice without the neomycin resistance gene).

for genomic DNA quantification with PicoGreen fluorescent dye (Invitrogen, Carlsbad, CA, USA). A prepared spike mRNA cocktail solution containing known quantity of five mRNAs of bacillus subtilis was added to the tissue lysate in proportion to the DNA quantity. Total RNA was purified from the lysate using the RNeasy kit (Qiagen). One microgram of total RNA was reverse-transcribed with SuperScript II (Invitrogen). Quantitative real time PCR was performed with an ABI PRISM 7900 HT sequence detection system (Applied Biosystems) using SYBR Green PCR Master Mix (Applied Biosystems), with initial denaturation at 95°C for 10 min followed by 40 cycles of 30 sec at 95°C and 30 sec at 60°C and 30 sec at 72°C, and Ct values were obtained. Primers for Cyp3a11 were Cyp3a11 FW and Cyp3a11 RV. Primers for Ces6 were Ces6 FW and Ces6 RV. Primers for mouse SXR selective quantification were mouse SXR FW and mouse SXR RV. Primers for hSXRki selective quantification were human SXR FW and human SXR RV. Primers for both mouse SXR and hSXRki quantification were mouse-human SXR FW and mouse-human SXR RV that amplify the DBD region of the chimera.

In Situ Hybridization analysis

Digoxigein-labeled cRNA probe for Cyp3a11 was synthesized according to Suzuki *et al.* (2005) by RT-PCR using mouse liver cDNA as a template. The primers used were as follows: forward 5'-GATTGGTTTTGATGCCTGGT-3' and reverse 5'-CAAGAGCTCACATTTTTCATCA-3'. The amplified product was sequence confirmed and ligated with Block-iT T7-TOPO (Invitrogen) Linker, which contains the T7 promoter site. A secondary PCR was performed to generate the sense and antisense DNA templates. For antisense template, Block-iT T7 Primer and Cyp3a11 forward primer (or reverse primer for generation of sense DNA template), the same primer as for the first PCR amplification, were used. With these DNA templates, both sense and antisense digoxigenin-labeled riboprobes were synthesized using a DIG RNA labeling kit (Roche Diagnostics, Germany) according to the manufacturer's protocol.

ISH on paraffin sections was carried out according to Suzuki *et al.* with a modification; permeabilization condition 98°C for 15 min in HistoVT One (Nacalai tesque, Japan).

Animals experiments

Male hSXRki and WT mice were maintained under a 12 hr light/12 hr dark cycle with water and chow (CRF-1, Oriental Yeast Co. Ltd., Tokyo, Japan) provided *ad libitum*. The animal studies were conducted in accordance with the Guidance for Animal Studies of the National Institute of Health Sciences under Institutional approval. The expression level of the hSXRki and WT SXR mRNA of ten organs (brain, thymus, heart, lung, liver, stomach, spleen, kidney, small intestine and testis) were analyzed on 15 weeks old male mice (n = 2) by the Percellome quantitative RT-PCR.

For the demonstration of selective gene induction by RIF and PCN in hSXRki and WT male mice on 13 weeks

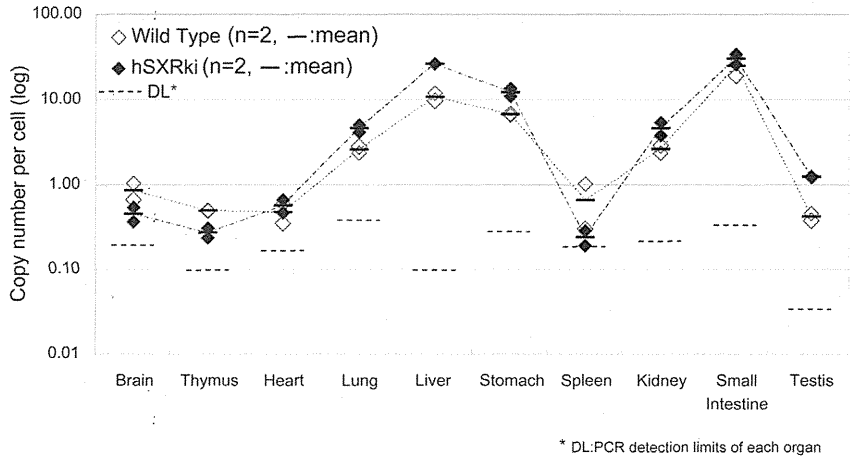

Fig. 2. Conservation of tissue expression patterns of hSXRki mRNA in the knock-in mouse. Percellome quantitative RT-PCR analysis was performed to measure the absolute expression levels of WT SXR mRNA and hSXRki mRNA in ten organs of WT and hSXRki mice. The expression levels of hSXRki mRNA among organs were comparable to WT.

old, three mice per group were singly dosed orally with vehicle (corn oil+0.1% DMSO), 10, 30, or 100 mg/kg of RIF, or 20, 70, or 200 mg/kg PCN (approximately equivalent in molar dose). Eight hours later, mice were sacrificed by exsanguination under ether anesthesia and the liver and the small intestine mucosa were sampled. Liver samples in small pieces were stored in RNA later (Applied Biosystems, Foster City, CA, USA) for further analysis. The small intestine under ice-cooled condition was longitudinally opened, gently rinsed with RNase-free saline and the epithelium was scraped with a glass slide and immersed in RNAlater. For *in situ* hybridization (ISH) of Cyp3a11 in the liver, 15 weeks old male hSXRki and WT mice were dosed orally with vehicle (corn oil), RIF (10 mg/kg), or PCN (40 mg/kg) daily for 3 days and liver sampled 24 hr later. All mice were sacrificed by exsanguination under ether anesthesia.

Statistical analysis

All values are expressed as the means ± S.D. and group differences analyzed by unpaired Student's *t* test or one-way ANOVA followed by Dunnett's post hoc comparison. Level of significance was set at $p < 0.05$.

RESULTS

Generation of hSXRki knock-In mice

Among 144 neomycin resistant TT2 ES clones, six PCR positive clones were further submitted to Southern blotting for the confirmation of homologous recombination. As shown in Fig. 1C, five clones were confirmed, and two (#4 and #25) were used to generate chimeric mice. The resulting mice were backcrossed to ICR strain to confirm germline transmission. One clone (#4) was crossed to a mouse constitutively expressing Cre recombinase to remove the neomycin resistance gene (Fig. 1D) and backcrossed to C57BL/6 CrSlc for at least 6 generations before further analysis.

Tissue distribution of hSXRki mRNA

Ten tissues, i.e., brain, thymus, heart, lung, liver, stomach, spleen, kidney, small intestine and testis from both hSXRki and WT mice were measured for hSXRki or WT SXR mRNA expression by the Percellome quantitative RT-PCR. As shown in Fig. 2, the levels of hSXRki mRNA are comparable to that of SXR in WT mouse and expressed in all tissues analyzed.

Humanized responses in hSXRki mouse

Humanized response of hSXRki was demonstrated by administration of the mouse-specific ligand PCN and the

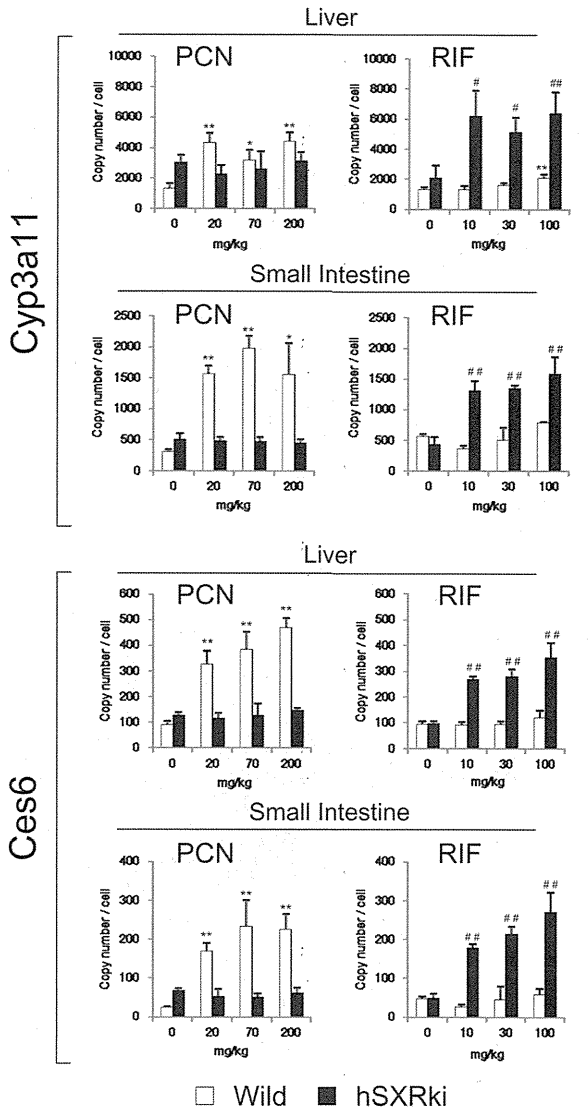

Fig. 3. Humanized response of hSXRki mice to RIF and PCN; Percellome quantitative RT-PCR. WT mice and hSXRki mice (n = 3 each) were singly dosed orally with vehicle (corn oil+0.1% DMSO), 20, 70, or 200 mg/kg PCN, or 10, 30, or 100 mg/kg of RIF (approximately equivalent in molar dose each other). Percellome quantitative RT-PCR data of Cyp3a11 and Ces6, both known as SXR target genes, in liver and small intestinal mucosa showed humanized responses in hSXRki. Bars = S.D., *; $p < 0.05$, **; $p < 0.01$ compared with vehicle group of WT, #; $p < 0.05$, ##; $p < 0.01$ compared with vehicle group of hSXRki. Analyzed by one-way ANOVA followed by Dunnett's post hoc comparison. Level of significance was set at $p < 0.05$.

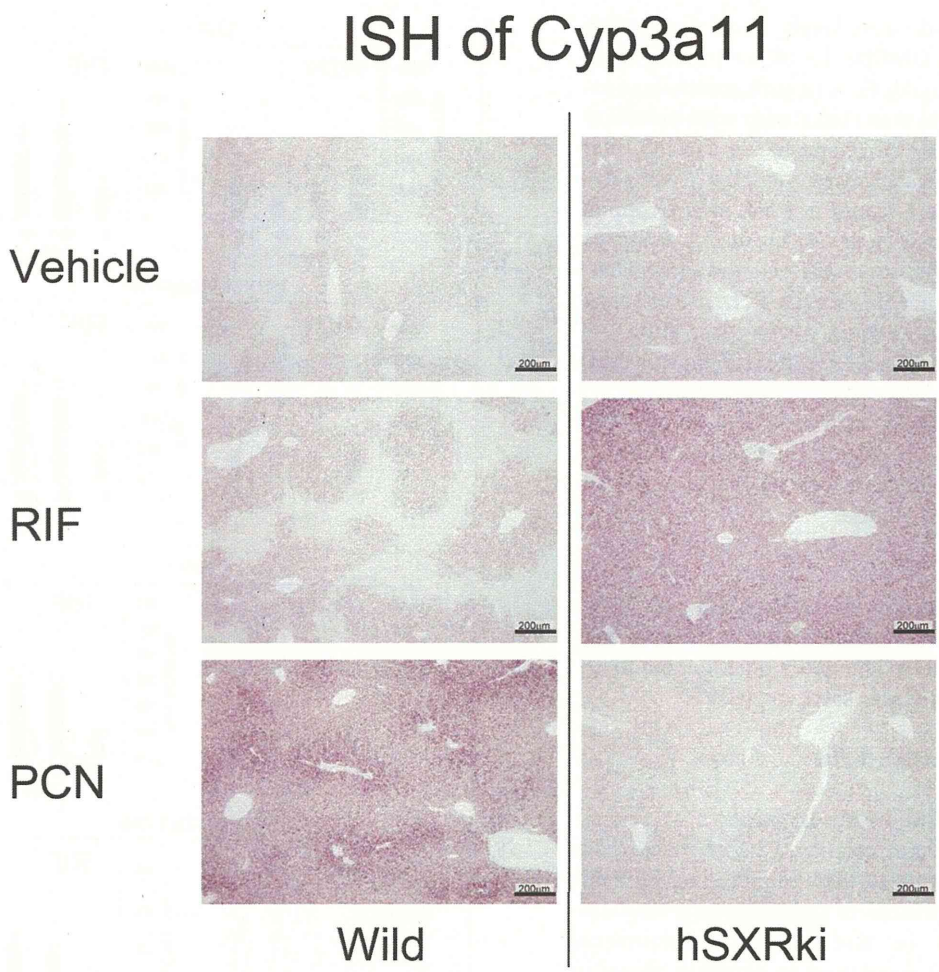

Fig. 4. Humanized response of hSXRki mice to RIF and PCN; *In situ* hybridization for Cyp3a11 mRNA in liver. A DIG-labeled cRNA probe for Cyp3a11 was hybridized and developed for purplish blue chromogenic reaction. Histologically, Cyp3a11 induction was localized around the central veins in both mice with species-specific ligands, respectively.

human-specific ligand RIF to the mice. Induction of the well-known SXR-regulated genes, Cyp3a11 and Ces6 was monitored by Percellome quantitative RT-PCR. As shown in Fig. 3, in the liver and small intestinal mucosa, RIF, but not PCN, induced Cyp3a11 and Ces6 in hSXRki mice (closed column), whereas PCN exclusively induced these genes in WT mice (open column). ISH of Cyp3a11 of the liver also showed humanized responses in hSXRki mice (Fig. 4).

DISCUSSION

We generated a new humanized mouse model in which the ligand binding domain (LBD) of human SXR was homologously knocked-into the murine SXR gene so that systemic response induced by human-selective SXR ligands can be monitored in mice. Firstly, we showed that mRNA from this chimeric gene was expressed at appropriate levels in the same tissues as the endogenous mouse SXR gene in WT mice. Then the humanized response of the mouse was confirmed by monitoring its response to the human-selective activator RIF, and the lack of response to the rodent-selective activator PCN.

There are relatively few reports about the regulation of SXR expression to date. Aouabdi *et al.* (2006) reported the presence of a PPAR alpha binding site 2.2 kb upstream of the transcription start site in human SXR. This site corresponded to the induction site with clofibrate in the rat and they further confirmed its importance using human liver cancer cell line (Huh7). Jung *et al.* (2006) reported the presence of four FXR binding sites in intron 2 of the mouse SXR gene that were required for FXR regulation of SXR expression. This intron 2 region is completely intact in our hSXRki mouse. Therefore, the regulation by FXR should be preserved in our mice.

Compared to the previously generated humanized Alb-SXR, SXR BAC, and hSXR genome mice, we contend that our hSXRki mouse has an advantage because the human-mouse chimeric gene is expressed in the same tissues and at similar levels to endogenous SXR in WT mice under control of the mouse promoter. This feature would make this model suitable not only for systemic toxicity but also toxicity at various stages of development of the embryo and fetus, maturation of infant, and of senescence, where the *cis* and *trans* regulations might be critical in its regulation (Sarsero *et al.,* 2004) (Konopka *et al.,* 2009). Thus, we believe that our system has a broader application range for toxicological studies.

ACKNOWLEDGMENTS

The authors thank Ms. Yuko Matsushima, Mr. Masaki Tsuji, Ms. Maki Otsuka, Mr. Yusuke Furukawa, Mr. Kouichi Morita, Ms. Maki Abe, and Ms. Shinobu Watanabe for technical support. This study was supported in part by the Health Sciences Research Grants H19-Toxico-Shitei-001 from the Ministry of Health, Labour and Welfare, Japan.

REFERENCES

Aouabdi, S., Gibson, G. and Plant, N. (2006): Transcriptional regulation of the PXR gene: identification and characterization of a functional peroxisome proliferator-activated receptor alpha binding site within the proximal promoter of PXR. Drug Metab. Dispos., **34**, 138-144.

Bertilsson, G., Heidrich, J., Svensson, K., Asman, M., Jendeberg, L., Sydow-Bäckman, M., Ohlsson, R., Postlind, H., Blomquist, P. and Berkenstam, A. (1998): Identification of a human nuclear receptor defines a new signaling pathway for CYP3A induction. Proc. Natl. Acad. Sci., USA, **95**, 12208-12213.

Blumberg, B., Sabbagh, W.Jr., Juguilon, H., Bolado, J.Jr., van Meter, C.M., Ong, E.S. and Evans, R.M. (1998): SXR, a novel steroid and xenobiotic-sensing nuclear receptor. Genes. Dev., **12**, 3195-3205.

Jung, D., Mangelsdorf, D.J. and Meyer, U.A. (2006): Pregnane X receptor is a target of farnesoid X receptor. J. Biol. Chem., **281**, 19081-19091.

Kanno, J., Aisaki, K., Igarashi, K., Nakatsu, N., Ono, A., Kodama, Y. and Nagao, T. (2006): "Per cell" normalization method for mRNA measurement by quantitative PCR and microarrays. BMC genomics, **7**, 64.

Konopka, G., Bomar, J.M., Winden, K., Coppola, G., Jonsson, Z.O., Gao, F., Peng, S., Preuss, T.M., Wohlschlegel, J.A. and Geschwind, D.H. (2009): Human-specific transcriptional regulation of CNS development genes by FOXP2. Nature, **462**, 213-217.

Lehmann, J.M., McKee, D.D., Watson, M.A., Willson, T.M., Moore, J.T. and Kliewer, S.A. (1998): The human orphan nuclear receptor PXR is activated by compounds that regulate CYP3A4 gene expression and cause drug interactions. J. Clin. Invest., **102**, 1016-1023.

Ma, X., Shah, Y., Cheung, C., Guo, G.L., Feigenbaum, L., Krausz, K.W., Idle, J.R. and Gonzalez, F.J. (2007): The PREgnane X receptor gene-humanized mouse: a model for investigating drug-drug interactions mediated by cytochromes P450 3A. Drug Metab. Dispos., **35**, 194-200.

Saga, Y., Hata, N., Koseki, H. and Taketo, M.M. (1997): Mesp2: a novel mouse gene expressed in the presegmented mesoderm and essential for segmentation initiation. Genes. Dev., **11**, 1827-1839.

Saga, Y., Miyagawa-Tomita, S., Takagi, A., Kitajima, S., Miyazaki, J. and Inoue, T. (1999): MesP1 is expressed in the heart precursor cells and required for the formation of a single heart tube. Development, **126**, 3437-3447.

Sakai, K. and Miyazaki, J. (1997): A transgenic mouse line that retains Cre recombinase activity in mature oocytes irrespective of the cre transgene transmission. Biochem. Biophys. Res. Commun., **237**, 318-324.

Sarsero, J.P., Li, L., Holloway, T.P., Voullaire, L., Gazeas, S., Fowler, K.J., Kirby, D.M., Thorburn, D.R., Galle, A., Cheema, S., Koenig, M., Williamson, R. and Ioannou, P.A. (2004): Human BAC-mediated rescue of the Friedreich ataxia knockout mutation in transgenic mice. Mamm. Genome., **15**, 370-382.

Scheer, N., Ross, J., Rode, A., Zevnik, B., Niehaves, S., Faust, N. and Wolf, C.R. (2008): A novel panel of mouse models to evaluate the role of human pregnane X receptor and constitutive androstane receptor in drug response. J. Clin. Invest., **118**, 3228-3239.

Suzuki, T., Akimoto, M., Mandai, M., Takahashi, M. and Yoshimura, N. (2005): A new PCR-based approach for the preparation of RNA probe. J. Biochem. Biophys. Methods., **62**, 251-258.

Tirona, R.G., Leake, B.F., Podust, L.M. and Kim, R.B. (2004): Identification of amino acids in rat pregnane X receptor that determine species-specific activation. Mol. Pharmacol., **65**, 36-44.

Watkins, R.E., Wisely, G.B., Moore, L.B., Collins, J.L., Lambert, M.H., Williams, S.P., Willson, T.M., Kliewer, S.A. and Redinbo, M.R. (2001): The human nuclear xenobiotic receptor PXR: structural determinants of directed promiscuity. Science, **292**, 2329-2333.

Xie, W., Barwick, J.L., Downes, M., Blumberg, B., Simon, C.M., Nelson, M.C., Neuschwander-Tetri, B.A., Brunt, E.M., Guzelian, P.S. and Evans, R.M. (2000): Humanized xenobiotic response in mice expressing nuclear receptor SXR. Nature, **406**, 435-439.

Yagi, T., Tokunaga, T., Furuta, Y., Nada, S., Yoshida, M., Tsukada, T., Saga, Y., Takeda, N., Ikawa, Y. and Aizawa, S. (1993): A novel ES cell line, TT2, with high germline-differentiating potency. Anal. Biochem., **214**, 70-76.

Zhou, C., Tabb, M.M., Sadatrafiei, A., Grün, F. and Blumberg, B. (2004) Tocotrienols activate the steroid and xenobiotic receptor, SXR, and selectively regulate expression of its target genes. Drug Metab. Dispos., **32**, 1075-1082.

Biol Trace Elem Res (2012) 145:166–171
DOI 10.1007/s12011-011-9180-0

Analysis of Trace and Major Elements in Bronchoalveolar Lavage Fluid of Mycoplasma Bronchopneumonia in Calves

Kazuyuki Suzuki · Hidetoshi Higuchi · Hidetomo Iwano · Jeffrey Lakritz · Kouichiro Sera · Masateru Koiwa · Kiyoshi Taguchi

Received: 30 May 2011 / Accepted: 12 August 2011 / Published online: 26 August 2011

Abstract The aim of this study was to evaluate the reliability and effectiveness of direct determination of trace and major element concentrations in bronchoalveolar lavage fluid samples from Holstein calves with *Mycoplasma* bronchopneumonia (n=21) and healthy controls (n=20). The samples were obtained during bronchoscopy using a standard examination method. A total of 18 elements (aluminum, bromine, calcium, chlorine, chromium, copper, iron, potassium, magnesium, manganese, molybdenum, nickel, phosphorous, sulfur, silicon, strontium, titanium, and zinc) were detected by particle-induced X-ray emission. The average bromine, iron, potassium, magnesium, and phosphorous concentrations were higher in calves with bronchopneumonia than in controls ($p<0.05$). They were found to have higher amounts of calcium and zinc, and a higher zinc–copper ratio than that in healthy calves ($p<0.001$). Based on the receiver operating characteristics curves, we propose a diagnostic cutoff point for zinc–copper ratio for identification of *Mycoplasma* pneumonia of 8.676. Our results indicate that assessment of the elemental composition of broncholaveolar lavage fluid is a promising diagnostic tool for *Mycoplasma* bronchopneumonia.

Keywords Bronchoalveolar lavage fluid · Calf · Trace elements · *Mycoplasma* bronchopneumonia · PIXE

Abbreviations

BALF	Bronchoalveolar lavage fluid
MMP	Matrix metalloproteinase
PCR	Polymerase chain reaction
PIMs	Pulmonary intravascular macrophages
PIXE	Particle-induced X-ray emission
ROC	Receiver operating characteristic

Introduction

Mycoplasma bovis is an important cause of calf pneumonia worldwide. Because immune prophylaxis and treatment with antibiotics are not very effective, control measures must include the introduction of strict hygiene standards, confinement of infected herds, and culling of clinically diseased animals [1]. Infection by *M. bovis* may develop into a severe suppurative bronchopneumonia or necrotizing pneumonia when associated with other organisms or, conversely, into a mild catarrhal broncho-interstitial pneumonia when associated with other microorganisms [2]. Pulmonary lesions in naturally infected calves comprise an exudative bronchopneumonia and extensive foci of coagulative necrosis surrounded by inflammatory cells [2]. Chronic infections are often associated with a lymphocytic "cuffing" pneumonia with marked hyperplasia of peribronchial lymphoid tissue that causes stenosis of the airway lumen and compression and collapse of adjacent pulmonary parenchyma [1].

K. Suzuki (✉) · H. Higuchi · H. Iwano · M. Koiwa · K. Taguchi
School of Veterinary Medicine, Rakuno Gakuen University,
582 Midorimati, Bunnkyoudai,
Ebetsu, Hokkaido 069-8501, Japan
e-mail: kazuyuki@rakuno.ac.jp

K. Suzuki · J. Lakritz
College of Veterinary Medical Science, Ohio State University,
601 Vernon L. Tharp St.,
Columbus, OH 43210-1089, USA

K. Sera
Cyclotron Research Center, Iwate Medical University,
Tomegamori,
Takizawa, Iwate 020-0173, Japan

Pulmonary intravascular macrophages (PIMs) are present in ruminants and horses [3]. These species are highly sensitive to acute lung inflammation compared with non-PIM-containing species such as rats and humans. As the source of TNF-alpha, PIMs promote recruitment of inflammatory cells including IL-8-containing platelets to stimulate acute inflammation in lungs [3]. Lung injury in human and animals are associated with modifications of the extracellular matrix metabolism that lead to an accumulation of several elements and the development of organ fibrosis [3]. In inflamed lungs, matrix metalloproteinase (MMP)-9 is a key contributor to degradation of lung tissue and it potentiates activation of neutrophil chemotactic chemokines. MMP-9 is overexpressed in inflammatory pulmonary disorders of lung in human with adult respiratory distress syndrome [4]. Elevated levels of both serine proteinases and MMPs have been reported in bronchoalveolar lavage fluid (BALF) taken from humans with adult respiratory distress syndrome [4, 5], dogs with pulmonary eosinophilia [6] and horses with chronic obstructive pulmonary disease [7]. Lakritz et al. [8] indicated that gelatinases MMP-2 and MMP-9 were detected in BALF of healthy calves and that lipopolysaccharide-stimulated alveolar macrophages express MMP-9. In addition, an association between pneumonias attributable to *Pasteurella multocida* or *Mycoplasma bovirhinis* in calves and accumulation of MMP-9 in tracheobronchial lavage fluid has been reported [9]. MMPs are a family of zinc and calcium-dependent endopeptidases involved in remodeling and physiological homeostasis of extracellular matrix [10]. Therefore, it is important to investigate the relevance of bronchopneumonia and trace and major element status for food animal health care. However, no comparative studies are available on the trace and major elements status in BALF form calves with *Mycoplasma* bronchopneumonia.

Thus, the aim of this study was to investigate the concentrations and relationships between trace and major elements in BALF from calves with *Mycoplasma* bronchopneumonia. The receivers operating characteristic (ROC) curves were used to describe the performance of BALF in screening for *Mycoplasma* bronchopneumonia and to propose diagnostic cutoffs for calves.

Materials and Methods

All procedures were performed in accordance with the Guide for the Care and Use of Laboratory Animals of the School of Veterinary Medicine at Rakuno Gakuen University and the National Research Council [11].

Forty-one Holstein calves, 31 males and 10 females, aged 85.3±46.1 days old, were enrolled in this study. The health status of the animals was established on the basis of physical, biochemical, thoracic ultrasound, and radiological examinations. Twenty-one calves were isolated at the Rakuno Gakuen University Veterinary Teaching Hospital showing clinical signs such as coughing, nasal discharge, fever, and pulmonary wheezing sounds. As controls, 20 healthy calves with none of these clinical symptoms were kept at the School of Veterinary Medicine, Rakuno Gakuen University.

The BALF samples were obtained during bronchoscopic examination using a standard protocol described elsewhere [12–14]. Briefly, bronchoscopy was performed using a flexible video bronchoscope (Olympus VQ Type 6092A, Olympus Co., Tokyo, Japan) under sedation with 0.05 mg/kg of 2% xylazine solution. The tip of the bronchoscope was wedged into a position in a tracheal bronchus. Two hundred milliliters isotonic, sterile saline solution warmed to 37°C was instilled in 50 mL portions with a disposable plastic syringe and immediately re-aspirated. The first aliquot was discarded [14]. In this procedure, a recovery rate of at least 60% is required.

Sub-samples were cultivated and investigated by polymerase chain reaction (PCR) tests targeting the *M. bovis*, based on 16S rRNA genes [15]. Briefly, simplified PCR was performed in a total reaction volume of 20 μL containing 10 μL of 2× AmpdirectPlus (Shimadzu Co., Kyoto, Japan), 0.5 U of Nova taq TM Hot Start DNA polymerase (Novagen, UK), 5 pmol of a mycoplasma universal primer set (MycoAce; Nihon Dobutsu Tokusyu Shindan Ltd., Hokkaido, Japan), and 5 μL of each samples. PCR was performed in an iCycler PCR System (Bio-Rad Laboratories, USA). Conditions for the simplified PCR were as follows: initial denaturation at 95°C for 10 min followed by 35 cycles of denaturation at 94°C for 30 s, annealing at 60°C for 45 s, and extension at 72°C for 1 min. The PCR products were separated by electrophoresis on 1.5% (*w/v*) agarose gels, stained with ethidium bromide, and visualized with a UV trans-illuminator. The *M. bovis* strain (ATCC 25523) was used as positive standard.

The BALF was then centrifuged at 180×*g* for 10 min at 4°C to remove cell debris and the supernatant was stored at −80°C until assay. The mean concentrations of trace and major elements in BALF were detected by the particle-induced X-ray emission (PIXE) method. A detailed description of the experimental arrangement is shown elsewhere [13, 16]. Briefly, 100 μL BALF supernatants were placed on a subtlety Myler membrane and desiccated. The supernatants were directly irradiated with proton beams. A small (baby) cyclotron used for positron nuclear medicine at the Nishina Memorial Cyclotron Center (Iwate, Japan) provides a 2.9-MeV proton beam on a target after passing through a graphite beam collimator. A Si (Li) detector (0.0254 mm Be window) with 300 and 1,000-μm thick Mylar absorbers was used to select X-rays with energy higher than that of K–K alpha. For lower-energy X-rays, another Si (Li) detector (0.008 mm Be) was used without absorber.

The data are shown as means±standard deviation (SD). Statistical analyses were performed using a commercial software package from IBM SPSS Statistics, v.19 (IBM Co, Somers, NY, USA). The mean values for each dependent variable were compared to the control values using the unpaired Student's t test after analysis of ANOVA as F test. The ROC curves were used to characterize the sensitivity and specificity of a parameter to *Mycoplasma* bronchopneumonia. The optimal cutoff point for a test was calculated by the Youden index [17]. The Youden index (J) is defined as the maximum vertical distance between the ROC curve and the diagonal or chance line and is calculated as J=maximum [sensitivity+specificity−1]. The cutoff point on the ROC curves that corresponds to J is taken to be the optimal cutoff point [17]. The significance level was set at $p<0.05$.

Results

Figure 1 shows the detection of *M. bovis* by simplified PCR based on 16S rRNA genes. The PCR for *Mollicutes* detected *M. bovis* in only one sample (5%) from a healthy calves (controls, n=20) and in all samples (n=21, 100%) from calves with bronchopneumonia. Therefore, the statistical analysis enrolled 19 healthy controls that had not detected *M. bovis* and 21 bronchopneumonia calves.

The mean concentrations of trace and major elements in BALF from calves with *Mycoplasma* bronchopneumonia are summarized in Table 1. The PIXE method allowed detection of 18 elements: Al, Br, Ca, Cl, Cr, Cu, Fe, K, Mg, Mn, Mo, Ni, P, S, Si, Sr, Ti, and Zn. The average concentrations of Br, Fe, K, Mg, and P were higher in the calves with bronchopneumonia than those of the controls ($p<0.05$). Additionally, the calves with *Mycoplasma* bronchopneumonia were found to have larger amounts of Ca and Zn compared to those without respiratory disease ($p<0.01$ and $p<0.001$, respectively). There are no significant differences in the levels of the remaining 11 elements.

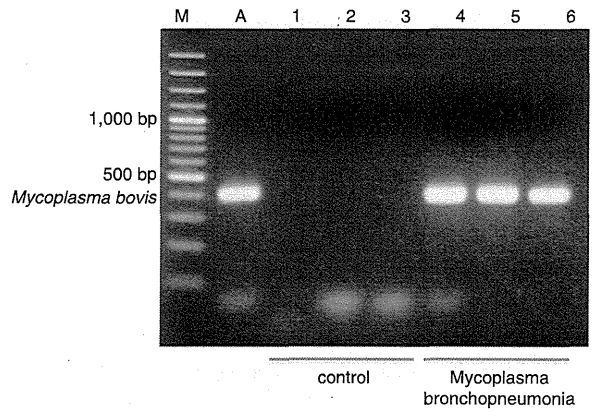

Fig. 1 Detection of *Mycoplasma bovis* in calves by polymerase chain reaction based on 16S rRNA genes. *M* marker, *A* positive standard (ATCC 25523), *lanes 1–3* control, and *lanes 4–6* bronchopneumonia calves

Table 1 Comparison of 18 trace and major elements status measured in broncoalveolar lavage fluid of the calves with or without *Mycoplasma* bronchopneumonia

(μg/mL)	Control (n=19)	*Mycoplasma* pnuemonia (n=21)	p value
Al	0.365[a]±0.238	0.942±0.924	NS[b]
Br	0.409±0.203	1.010±0.814	$p<0.05$
Ca	4.78±1.62	10.05±6.92	$p<0.01$
Cl	704.3±176.4	1,110.4±874.0	NS
Cr	0.028±0.016	0.038±0.021	NS
Cu	0.026±0.036	0.034±0.040	NS
Fe	0.099±0.070	0.201±0.190	$p<0.05$
K	34.4±12.5	65.3±32.9	$p<0.05$
Mg	1.13±0.75	3.11±2.39	$p<0.05$
Mn	0.012±0.008	0.014±0.016	NS
Mo	0.052±0.036	0.029±0.025	NS
Ni	0.009±0.005	0.007±0.005	NS
P	3.21±1.89	15.33±10.45	$p<0.05$
S	8.62±2.26	27.35±21.23	NS
Si	1.19±0.68	1.93±1.09	NS
Sr	0.017±0.015	0.016±0.016	NS
Ti	0.094±0.085	0.124±0.058	NS
Zn	0.074±0.048	0.366±0.166	$p<0.001$
Ca/P	2.01±1.63	1.01±0.66	NS
Zn/Cu	5.93±5.48	26.84±19.57	$p<0.001$

[a] micrograms per liter (μg/mL)

[b] Not significant

The areas under the ROC curves for Ca and Zn concentrations were 0.779 ($p<0.01$) and 0.990 ($p<0.001$), respectively (Fig. 2). The proposed diagnostic cutoff points for Ca and Zn concentrations in BALF for identifying *Mycoplasma* bronchopneumonia based on the analysis of the ROC curves were set at 5.894 and 0.180 μg/mL, respectively. Sensitivities and specificities of proposed diagnostic cutoffs for Ca concentration in BALF were 71.4% and 90.0%, respectively. In the same manner, sensitivities and specificities of proposed diagnostic cutoffs for Zn concentration in BALF were 95.2% and 95.0%, respectively.

Figure 3 shows a ROC curves for Zn/Cu ration in detecting *Mycoplasma* bronchopneumonia in calves. In the body, Ca and P, and Zn and Cu are regulated and restricted by each other, so variations in the Ca/P and the Zn/Cu ratios reflect the effects of these two microelements, respectively [13, 16]. However, in the calves with *Mycoplasma* bronchopneumonia, no characteristic difference of the Ca/P ratio was found in BALF. In contrast, the Zn/Cu ratios of

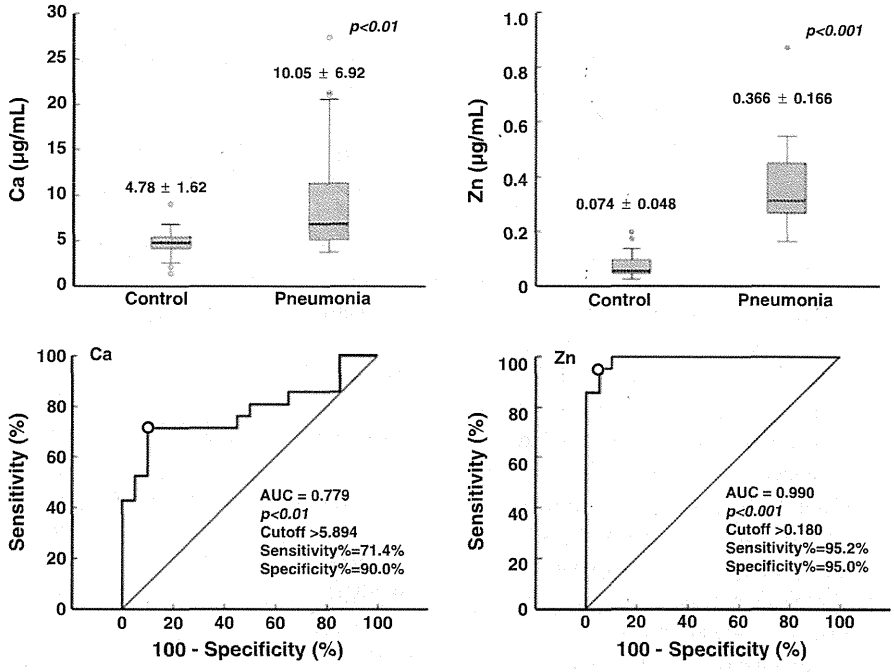

Fig. 2 Receiver operating characteristic (ROC) curves for Ca and Zn concentrations for detection of *Mycoplasma* bronchopneumonia in calves. The mean area under the ROC curve (AUC) is shown for each ROC curve. The optimal cutoff point for test was calculated by the Youden index. *Open circle* cutoff point

the BALF in the calves with *Mycoplasma* bronchopneumonia (26.84±19.57) were significantly higher than that of the healthy control (4.91±3.48, $p<0.001$). Proposed diagnostic cutoff points for Zn/Cu ratios in BALF for identifying *Mycoplasma* pneumonia based on the analysis of the ROC curves were set at 8.676. Sensitivities and specificities of proposed diagnostic cutoffs for Zn/Cu ratio in BALF were 93.8% and 82.4%, respectively.

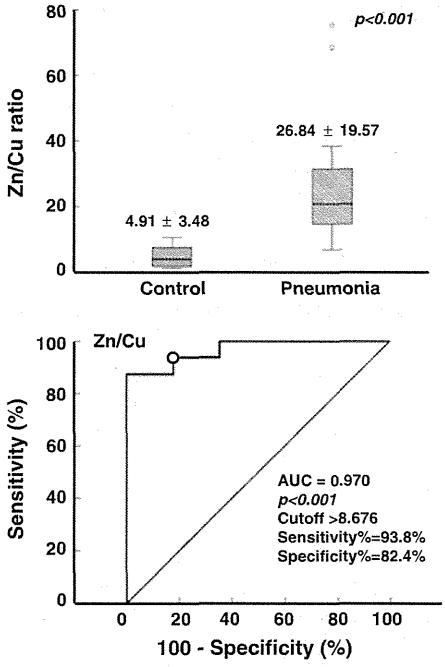

Fig. 3 Receiver operating characteristic (ROC) curves for the Zn/Cu ratio for detection of *Mycoplasma* bronchopneumonia in calves. See Fig. 2 for key

Discussion

We found how *Mycoplasma* bronchopneumonia in calves is associated with the concentrations of some trace and major elements in BALF. The calves with *Mycoplasma* bronchopneumonia were found to have larger concentrations of Br, Ca, Fe, K, Mg, P and Zn, and a high Zn/Cu ratio in BALF compared to those without bronchopneumonia. In addition, the proposed diagnostic cutoffs for Ca and Zn concentrations and Zn/Cu ratio in BALF based on ROC curves analysis in detecting a *Mycoplasma* bronchopneumonia were set at 5.894 and 0.180 μg/mL, and 8.676, respectively.

The clinical and pathological signs for bronchopneumonia caused by *M. bovis* are non-specific, so laboratory diagnosis is necessary for identification of the disease. To that effect, PCRs have been used to detect *M. bovis* directly in milk and nasal samples [18]. Several researches demonstrated that sampling by BALF was more useful for prediction of lower respiratory airway pathogens than nasal swabs although clearly not as convenient [19, 20]. Therefore, in this study, PCRs based on 16S rRNA genes amplified *M. bovis* DNA [15, 21] and were used to confirm *Mycoplasma* bronchopneumonia, using BALF samples.

The PIXE method used in the present study is a fast and reliable multi-element qualitative and quantitative analytical tool that is easily accomplished [22]. In this technique, a

detector analyzes characteristic X-rays emitted as a result of inner-shell ionization of target atoms. The method works well in small samples and is suitable for determining elements in a solid surface, especially for analyzing medium and higher atomic weight elements in a matrix consisting of light elements. With this technique, a sample of a few micrograms is sufficient to analyze concentrations in the parts-per-million range [22]. Because the method does not involve complicated sample preparation, the risk of contamination during the preparation of a sample for PIXE method is remarkably lower than that for other methods [13, 16].

Our results show that the average Br, Fe, K, Mg, and P concentrations in BALF from bronchopneumonia calves were higher than those in controls. A structurally and functionally distinct enzyme from neutrophil myeloperoxidase has the unique ability to use halides or pseudohalides (X^-) and H_2O_2 derived from the respiratory burst to generate cytotoxic hypohalous acids, especially hypobromous acid (HOBr) [23, 24]. The eosinophil peroxidase (EPO), such as EPO–H_2O_2–Br^- system, is also an effective cytotoxin for multiple targets such as multicellular worms or parasites, bacteria, viruses, and host cells [23]. Both HOBr and the EPO–H_2O_2–Br^- system are involved in many of the pathophysiological features of inflamed respiratory disease [24].

Iron is involved in many enzymatic activities. Significant changes in Fe concentration have been reported in BALF of patients with acute respiratory distress syndrome [25]. These changes have been interpreted as indicating that lungs require basal levels of extracellular redox-active Fe [26].

Potassium, magnesium, and phosphorus leak out to the extracellular fluid from tracheal epithelial cell injury because these elements are mostly contained in the intracellular fluid. Majeschak et al. [27] suggested that the Mg^{2+}/ATP-dependent 26S proteasome complex exists outside the cell and is released into the lung epithelial lining fluid after lung injury and contributes to the proteolysis of the bulk of protein in the alveolar space. BAL phospholipid content in lung injury rats correlated with the severity of alveolar-capillary leak [3]. Therefore, increased levels of Br, K, Fe, Mg, and P in BAL might be highly correlated with bronchial inflammation caused by *M. bovis*.

It was also found that BALF from calves with *Mycoplasma* bronchopneumonia were found to have larger concentrations of Ca and Zn and a high Zn/Cu ratio compared to those without respiratory disease. It is known that a calcium ionophore induces airway hyper-responsiveness to intravenous histamine and substance P possibly by reducing the nitric oxide levels in the airway tissues. This may be due to damaged airway epithelium and/or NO breakdown by activated inflammatory cells in the airway [28]. It is speculated that there is a correlation between Ca levels in BALF and the damage of the airway epithelium in calves with *Mycoplasma* bronchopneumonia. MMPs are a family of Zn and Ca-dependent endopeptidases involved in remodeling and physiological homeostasis of the extracellular matrix, shown to be important in the early stages of inflammation associated with respiratory disease in cattle [8, 29].

Associations between pneumonias attributable to *P. multocida* or *M. bovirhinis* in calves and accumulation of MMP-9 in tracheobronchial lavage fluid have been reported [9]. These molecules have high Zn-binding ability, containing three Zn-binding histidines and a glutamate that acts as a general base/acid during catalysis [30]. Furthermore, MMPs have three α-helices and a five-stranded β-sheet, as well as at least two Ca sites and a second Zn site with structural functions. Consequently, MMPs depend upon ionized Zn for activity and on Ca for stability. The changes of these elements are not specific with *Mycoplasma* bronchopneumonia because they result from reactions to inflammation of the bronchus and the tracheal branches. However, *Mycoplasma* bronchopneumonia induces severe airway inflammation accompanied by profound and persistent micro-vascular remodeling in tracheobronchial mucosa. The present results support these findings.

The pathogenesis of *Mycoplasma* bronchopneumonia is usually studied by genetic, proteomic, or molecular biology approaches. This study suggests that direct determination of trace and major elements concentrations in BALF could be a useful approach to the study of the pathogenesis of *Mycoplasma* bronchopneumonia. Infected calves were found to have higher amounts of Ca and Zn and a high Zn/Cu ratio in BALF compared to those without respiratory disease.

In conclusion, it is suggested that measuring the Br, Ca, Fe, K, Mg, P, and Zn concentrations and the Zn/Cu ratio status in BALF might help with diagnosis and even predict the susceptibility of a calf to *Mycoplasma* bronchoneumonia. Future studies need to focus in determining whether there is a correlation between zinc and calcium levels in BALF and the severity of bronchopneumonia.

Acknowledgments This study was supported by a grant-in-aid for Science Research from the Ministry of Education, Culture and Sciences of Japan (no.21580393) awarded to K. Suzuki and by a grant from Rakuno Gakuen University Research to K. Suzuki.

References

1. Nicholas RA, Ayling RD, McAuliffe L (2009) Vaccines for *Mycoplasma* diseases in animals and man. J Comp Pathol 140 (2–3):85–96
2. Radaelli E, Luini M, Loria GR et al (2008) Bacteriological, serological, pathological and immunohistochemical studies of *Mycoplasma bovis* respiratory infection in veal calves and adult cattle at slaughter. Res Vet Sci 85(2):282–290
3. Singh B, Pearce JW, Gamage LN et al (2004) Depletion of pulmonary intravascular macrophages inhibits acute lung inflammation. Am J Physiol Lung Cell Mol Physiol 286(2):L363–L372

4. Parks WC, Shapiro SD (2001) Matrix metalloproteinases in lung biology. Respir Res 2:10–19
5. Torii K, Iida K, Miyazaki Y et al (1997) Higher concentrations of matrix metalloproteinases in bronchoalveolar lavage fluid of patients with adult respiratory distress syndrome. Am J Respir Crit Care Med 155:43–46
6. Rajamäki MM, Järvinen AK, Sorsa T et al (2002) Clinical findings, bronchoalveolar lavage fluid cytology and matrix metalloproteinase-2 and -9 in canine pulmonary eosinophilia. Vet J 163:168–181
7. Hobo T, Yoshihara M, Oikawa M et al (2001) Surfactant proteins in bronchoalveolar lavage fluid of horses: assay technique and changes following road transport. Vet Rec 148:74–80
8. Lakritz J, Marsh AE, Cockrell M et al (2004) Characterization of gelatinases in bronchoalveolar lavage fluid and gelatinases produced by alveolar macrophages isolated from healthy calves. Am J Vet Res 65:163–172
9. Simonen-Jokinen TL, Eskelinen UM, Hartel HM et al (2005) Gelatinolytic matrix metalloproteinases-2 and -9 in tracheobronchial lavage fluid obtained from calves with concurrent infections of *Pasteurella multocida* and *Mycoplasma bovirhinis*. Am J Vet Res 66:2101–2106
10. Birkedal-Hansen H (1995) Proteolytic remodeling of extracellular matrix. Curr Opinion Cell Biol 7:728–735
11. National Research Council (1996) Guide for the Care and Use of Laboratory Animals. National Academy Press, Washington, DC, pp 1–70
12. Bargagli E, Monaci F, Bianchi N et al (2008) Analysis of trace elements in bronchoalveolar lavage of patients with diffuse lung diseases. Biol Trace Elem Res 124(3):225–235
13. Suzuki K, Yamaya Y, Kanzowa N et al (2008) Trace and major elements status in bronchoalveolar lavage fluid in dogs with or without bronchopneumonia. Biol Trace Elem Res 124:92–96
14. Schildge J, Nagel C, Grun C (2007) Bronchoalveolar lavage in interstitial lung diseases: does the recovery rate affect the results? Respiration 74:553–557
15. Higuchi H, Iwano H, Kawai K et al (2011) A simplified PCR assay for fast and easy *Mycoplasma* mastitis screening in dairy cattle. J Vet Sci 12(2):191–193
16. Asano K, Suzuki K, Chiba M et al (2005) Correlation between 25 element contents in mane hair in riding horses and atrioventricular block. Biol Trace Elem Res 108:127–136
17. Akobeng AK (2007) Understanding diagnostic tests 3: receive operating characteristic curves. Acra Paediatrica 96:644–647
18. Hotzel H, Sachse K, Pfützner H (1996) Rapid detection of *Mycoplasma bovis* in milk samples and nasal swabs using the polymerase chain reaction. J Appl Bacteriol 80(5):505–510
19. Nicholas RA, Ayling RD (2003) *Mycoplasma bovis*: disease, diagnosis, and control. Res Vet Sci 74(2):105–112
20. Thompson K, Molina R, Donaghey T et al (2006) The influence of high iron diet on rat lung manganese absorption. Toxicol Appl Pharmacol 210:17–23
21. Marques LM, Buzinhani M, Yamaguti M et al (2007) Use of a polymerase chain reaction for detection of *Mycoplasma dispar* in the nasal mucus of calves. J Vet Diagn Invest 19(1):103–106
22. Chiba M (1994) Bioinorganic chemistry: a science in the spotlight —interface of chemistry, biology, agriculture and medicine. International Journal of PIXE 4:201–216
23. Wu W, Samoszuk MK, Comhair SA et al (2000) Eosinophils generate brominating oxidants in allergen-induced asthma. J Clin Invest 105:1455–1463
24. Brottman GM, Regelmann WE, Slungaard A et al (1996) Effect of eosinophil peroxidase on airway epithelial permeability in the guinea pig. Pediatr Pulmonol 21:159–166
25. Gutteridge JM, Mumby S, Quinlan GJ et al (1996) Pro-oxidant iron is present in human pulmonary epithelial lining fluid: implications for oxidative stress in the lung. Biochem Biophys Res Commun 220:1024–1027
26. Gutteridge JM, Quinlan GJ, Evans TW (2001) The iron paradox of heart and lung and its implications for acute lung injury. Free Radic Res 35:439–443
27. Majeschak M, Sorell LT, Patricelli T et al (2009) Detection and possible role of proteasomes in the bronchoalveolar space of the injured lung. Physiol Res 58(3):363–372
28. Uno D, Tsukagoshi H, Hisada T et al (1997) Effects of the calcium ionophore A23187 on airway responsiveness to histamine and substance P in guinea pigs. Inflamm Res 46:108–113
29. Radi ZA, Kehrli ME Jr, Ackermann MR (2001) Cell adhesion molecules, leukocyte trafficking, and strategies to reduce leukocyte infiltration. J Vet Intern Med 15:516–529
30. Tallant C, Marrero A, Gomis-Rüth FX (2010) Matrix metalloproteinases: fold and function of their catalytic domains. Biochim Biophys Acta 1803(1):20–28

Zygote: page 1 of 6 © Cambridge University Press 2013
doi:10.1017/S0967199412000615

C-type natriuretic peptide inhibits porcine oocyte meiotic resumption

Yuki Hiradate[1], *Yumi Hoshino*[2], *Kentaro Tanemura*[2] *and Eimei Sato*[2]
Laboratory of Animal Reproduction, Graduate School of Agricultural Science, Tohoku University, Aobaku, Sendai, Japan

Date submitted: 05.07.2012. Date accepted: 10.09.2012

Summary

C-type natriuretic peptide (CNP) is a recently identified meiotic inhibitor in mice. However, it has not been investigated in porcine oocytes to date. This study aimed to demonstrate the inhibitory effect of CNP against germinal vesicle breakdown (GVBD) in porcine oocyte meiotic resumption. Immunohistochemical analysis revealed intense natriuretic peptide receptor 2 (NPR2) immunoreactivity in the oocyte surrounded cumulus cells in the follicles. Furthermore, reverse transcription polymerase chain reaction (RT-PCR) analysis showed the expression of *npr2* mRNA only in cumulus cells but not in oocytes, suggesting that cumulus cells are the targets of CNP. When cumulus–oocyte complexes (COCs) or denuded oocytes (DOs) were cultured with various concentrations of CNP (10, 50, 100, 500, and 1,000 nM), inhibitory effect was observed in the COC group, but not in the DO group, confirming that CNP indirectly inhibits GVBD via cumulus cells. This evidence is the first indication that the CNP-NPR2 pathway is involved in meiotic arrest in porcine oocytes. Furthermore, we investigated the effect of oocyte-derived paracrine factor (ODPF) on *npr2* mRNA expression level in cumulus cells by evaluating changes in mRNA expression in oocytectomised COCs (OXCs) by real-time PCR. A significant decrease in *npr2* mRNA expression level was observed in OXCs, whereas mRNA expression level was restored in OXCs with DOs, indicating that ODPF participates in the regulation of *npr2* expression in porcine cumulus cells.

Keywords: C-type natriuretic peptide, Germinal vesicle breakdown, Natriuretic peptide receptor 2, Oocytectomy, Porcine

Introduction

In the mammalian reproductive system, oocytes are arrested within ovarian follicles at the diplotene stage of the first meiotic prophase; this is termed as meiotic arrest. During meiotic arrest, the intact nuclear membrane forms a germinal vesicle characteristic of this phase. Once signal transduction is triggered by gonadotropin in cumulus cells surrounding the oocyte, germinal vesicle breakdown (GVBD) is induced by the closing of gap junctions and a decrease in intra-oocyte cAMP concentration in mice and pigs (Webb *et al.*, 2002; Fan *et al.*, 2004). Intriguingly, as mammalian oocytes cultured *in vitro* undergo GVBD, it has been suggested that an inhibitor of meiotic resumption is present *in vivo* (Pincus & Enzmann, 1935). Indeed, hypoxanthine isolated from porcine follicular fluid prevents oocyte maturation (Downs *et al.*, 1985). Hypoxanthine has been also found in follicular fluids from other species (Kadam & Koide, 1990), and induction of meiotic arrest by hypoxanthine has been observed in a wide range of species (Eppig & Downs, 1987; Warikoo & Bavister, 1989; Gotze *et al.*, 1990); hypoxanthine is considered one of the active meiotic inhibitors in mammalian ovary.

C-type natriuretic peptide (CNP) belongs to the natriuretic peptide family, which comprises three similar but genetically distinct peptides: atrial natriuretic peptide (ANP), brain natriuretic peptide (BNP), and CNP (Potter *et al*, 2006). These peptides have different affinities to their receptors. In contrast to ANP and BNP, which have high affinity to natriuretic

[1]All correspondence to Yuki Hiradate. Laboratory of Animal Reproduction, Graduate School of Agricultural Science, Tohoku University, Aobaku, Sendai 981–8555, Japan. Tel:/Fax: +81 22 717 8687. E-mail:hiradate@bios.tohoku.ac.jp
[2]Laboratory of Animal Reproduction, Graduate School of Agricultural Science, Tohoku University, 1-1 Tsutsumidori-Amamiyamachi, Aobaku, Sendai 981–8555, Japan.

peptide receptor 1 (NPR1), CNP has high affinity to natriuretic peptide receptor 2 (NPR2). The signature characteristic of natriuretic peptides is the production of cyclic guanosine monophosphate (cGMP), and their biological activities are mediated through a cGMP-dependent pathway. Several functions of natriuretic peptides have been reported, such as regulation of blood pressure (Woodard & Rosado, 2008) and natriuresis (Ballermann & Brenner, 1987).

Natriuretic peptides also play an important role in oocyte meiotic resumption. cGMP has been reported to be a crucial factor in maintaining meiotic arrest by entering into the oocyte through gap junctions and inhibiting the activity of oocyte phosphodiesterase 3, which hydrolyses cAMP in mice (Norris *et al.*, 2009). Törnell *et al.* (1990) have reported that ANP induces cGMP production in rat cumulus–oocyte complexes (COCs), and thereby inhibits spontaneous meiotic resumption. cGMP also acts as a GVBD inhibitor in porcine oocytes (Petr *et al.*, 2006), and the function of ANP as a meiotic inhibitor has also been reported. Recently, CNP has been reported to act as a meiotic inhibitor in mice (Zhang *et al.*, 2010). The report showed that cGMP produced in cumulus cells diffuses into oocytes through gap junctions and helps maintain the cAMP level in the oocytes, thereby preventing meiotic resumption. Histological analysis of *cnp*- and *npr2*-mutant mouse ovaries revealed that these models failed to maintain meiotic arrest, strongly suggesting the importance of the CNP-NPR2 pathway in oocyte maturation. However, the effect of CNP on porcine oocyte meiotic resumption was not determined. This study aims to demonstrate the effect of CNP on porcine oocyte meiotic resumption.

The present study also aims to investigate the regulation mechanism of CNP cognate receptor, *npr2*, in a porcine model. In the mouse model, *npr2* mRNA expression was regulated by oocyte-derived paracrine factors (ODPF). To demonstrate the effect of ODPF in the porcine model, we examined *npr2* mRNA expression in oocytectomised COCs (OXCs).

Materials and methods

Chemicals

The chemicals used in the study were obtained from Sigma-Aldrich unless stated otherwise.

Histological analysis of NPR2 localisation in porcine ovarian follicles

Porcine ovaries in prepubertal gilts were transected and fixed in a methacarn solution (methanol/chloroform/acetic acid, 6:3:1) for 48 h. After dehydration, the samples were embedded in paraffin and cut into 10-μm sections. The sections were kept until histological staining. For immunohistochemistry, deparaffinised sections were boiled for 25 min at 90°C to retrieve the antigen in HistoV (Nacalai Tesque, Kyoto, Japan). Then, the sections were treated with a blocking buffer (Blocking One; Nacalai Tesque) for 1 h at 4°C and with an antibody against NPR2 (Santa Cruz Biotechnology, diluted 1:10) overnight at 4°C. After being washed with phosphate-buffered saline (PBS), the sections were reacted with anti-goat Alexa 488-conjugated antibody (Molecular Probes, # A11078, Lot: 602–1, diluted 1:1,000) and propidium iodide (diluted 1:10,000) for 2 h at room temperature. The cells were observed under a confocal laser scanning microscope (LSM700; Zeiss, Jena, Germany).

In vitro maturation of porcine oocytes

Ovaries were collected at a local slaughterhouse and transported to the laboratory in warm saline (37°C). COCs were aspirated from ovarian follicles of 3- to 5-mm diameter with a 10-ml syringe attached to an 18-gauge needle. Twenty compact COCs with uniform ooplasm were selected in PBS supplemented with 0.1% (w/v) polyvinyl alcohol (PVA). After being washed in PBS-PVA, the 20 COCs were cultured in 200 μl of bovine serum albumin (BSA)-free North Carolina State University 23 (NCSU23) medium (Petters & Wells, 1993) supplemented with 50 μM β-mercaptoethanol, 0.6 mM cysteine (Sigma), 0.5% insulin, 10% (v/v) porcine follicular fluid, pregnant mare serum gonadotropin (10 IU/ml) (Serotropin; Teikokuzouki, Tokyo, Japan), and human chorionic gonadotropin (10 IU/ml) (Puberogen; Sankyo, Tokyo, Japan). The COCs were cultured at 38.5°C in 5% CO_2 in air with maximum humidity. Before analysis of the CNP effect on GVBD occurrence, COCs were pre-cultured in medium with 1 mM dibutyryl cyclic adenosine monophosphate (dbcAMP) for 22 h to synchronise nuclear maturation. After the 22-h pre-culture, denuded oocytes (DOs) were prepared from some of the incubated COCs by removing cumulus cells by pipetting. Then, the COC and DO groups were further cultured for 22 h in a medium without hormones and dbcAMP in the presence of various concentrations of CNP (10, 50, 100, 500, or 1000 nM). Each concentration of CNP was prepared as a 100× stock solution in PBS and added into the medium at the indicated final concentration. After 22 h of culture, cumulus cells were removed and oocytes in both groups were fixed in acetic acid/ethanol (1:3) for 48 h. Then, fixed oocytes were stained with 1% aceto-orcein and observed under a phase-contrast microscope to evaluate GVBD induction.

Oocytectomy of porcine COCs

Oocytectomy of oocytes was performed as described by Kimura *et al.* (2002). Briefly, a COC was fixed to the bottom of the dish with precision tweezers, and a puncture was made through the layer of cumulus cells and the oocyte with the tip of a 26-gauge needle. Then, the oocytoplasm was pressed out gradually with the tweezers. Twenty COCs, OXCs, or OXCs with DOs were cultured in 20 μl of NCSU23 medium without dbcAMP and hormones for 24 h.

RNA isolation and cDNA synthesis

After the COCs were cultured for the indicated periods, the oocytes and cumulus cells were separated from the COCs. Cumulus cells were removed from COCs with a glass pipette and transferred into a microtube, washed twice in PBS, and centrifuged at 1,000 rpm for 3 min. Total RNA was extracted from oocytes or cumulus cells with an RNeasy Micro Kit (Qiagen), following the manufacturer's instructions. Reverse transcription was performed in a 20-μl mixture containing 1 μl of cDNA and RNase inhibitor, 4 μl of 5× buffer and dNTP, 2 μl of dithiothreitol (DTT), and 1 μl of reverse transcriptase (SuperScript II; Invitrogen, Carlsbad, CA, USA). The mixture was then incubated at 42°C for 50 min and at 70°C for 15 min.

Reverse transcription-PCR

For detection of *npr2* mRNA in cumulus cells and oocytes, RT-PCR was performed. Specific primers for *npr2* and β-*actin* were designed with the following sequences: *npr2* (NCBI accession no. AY550069), ggcacaggaatcaccttcat (forward) and tgaagcgagtgagatggttg (reverse); β-*actin* (NCBI accession no. NM_001244322), aggtcatcactattggcaac (forward) and actcatcgtactcctgcttg (reverse) (Roh *et al.*, 2007). The generated product size for *npr2* and β-*actin* was 364 bp and 363 bp, respectively. The reaction volume was 20 μl, and *Taq* polymerase (Takara Bio, Otsu, Shiga, Japan) was used. cDNA was amplified using the following program: 35 cycles of denaturation at 95°C, annealing at 57°C for *npr2* or at 57.5°C for β-*actin*, and elongation at 72°C for 45 s).

Real-time PCR quantification

For quantitative analysis of *npr2* mRNA expression, real-time PCR was performed. Total RNA (250 ng) was reverse-transcribed. The specific primers were designed based on the sequences of *npr2* (forward: atggtcaacgccatgccccg, reverse: cccgtgtgcacccctatgcg) and β-*actin* (forward: atcgtgcgggacataag, reverse: ctcgttgccgatggtgat); product sizes of 123 and 251 bp, respectively, were generated. The program consisted of 44 cycles of denaturation at 94°C for 5 s, annealing at 61°C for 20 s, and extension at 72°C for 15 s, with additional extension at 72°C for 5 min. To confirm whether the correct gene was amplified, the obtained products were loaded onto 2% agarose gels and electrophoresed. The *npr2* mRNA expression levels were normalised to the β-*actin* level. The mean sample and endogenous control threshold cycles (Ct) for each sample were calculated with the ($2^{-\Delta\Delta Ct}$) method. The experiments were performed at least three times.

Statistical analysis

Each experiment was replicated three times. Statistical differences between the means of the two groups were analysed using Student's *t*-test. Differences between more than two groups were assessed by analysis of variance followed by a Bonferroni-Dunn test with STATVIEW (Abacus Concepts Inc., Berkeley, CA, USA). *P*-values less than 0.05 were considered to be significant. Data were represented as mean ± standard deviation (SD).

Results and Discussion

As shown in Fig. 1, intense NPR2 immunoreactivity was detected in oocyte surrounded cumulus cells, suggesting the presence of NPR2 in porcine ovarian follicles. We examined the expression of *npr2* mRNA in cumulus cells and oocytes by RT-PCR, and confirmed that *npr2* mRNA is expressed in porcine cumulus cells but not in oocytes (Fig. 2). This result suggests that CNP targets cumulus cells but not the oocytes. In order to demonstrate the hypothesis, oocytes with CNP were cultured *in vitro*. When COCs were cultured with CNP for 9 h after 22 h of pre-culture in medium containing dbcAMP, significant GVBD inhibition was observed at CNP concentrations of more than 10 nM (Fig. 3). In contrast, when DOs were cultured, CNP did not significantly inhibit the GVBD at any concentration. Our result clearly demonstrates that CNP also acts as a meiotic inhibitor in porcine oocytes. Because the bioreactivity of CNP is attributed to a cGMP-dependent cascade (Schulz, 2005), it seems that CNP-generated cGMP in cumulus cells is transported into the oocyte and that it plays an important role in meiotic arrest.

Npr2, the cognate receptor of CNP, is widely expressed, such as in aortic smooth muscle cells (Rahmutula & Gardner, 2005) or the spinal cord (Schmidt *et al.*, 2007). However, there is limited information about the role of CNP in the ovary. Jankowski *et al.* (1997) reported that *cnp* and *npr2* mRNA expression levels in the ovary are modulated by the oestrous cycle in a rat model. In addition, they